The effect of chitosan content on the crystallinity, thermal stability, and mechanical properties of bacterial cellulose–chitosan composites

Z Cai[1], **P Chen**[2], **H-J Jin**[2], and **J Kim**[1]*
[1]Center for EAPap Actuator, Department of Mechanical Engineering, Inha University, Republic of Korea
[2]Department of Polymer Science and Engineering, Inha University, Yonghyun-Dong, Nam-Ku, Incheon, Republic of Korea

The manuscript was received on 12 December 2008 and was accepted after revision for publication on 6 May 2009.

DOI: 10.1243/09544062JMES1480

Abstract: A bacterial cellulose–chitosan (BC–Chi) composite has been successfully prepared by immersing wet BC pellicle in chitosan acetic acid solution followed by freeze-drying. By changing chitosan concentration and immersion time, a foam-like structure is made with the chitosan content in the range of 12–45 per cent. Scanning electron microscope images show that chitosan molecules can penetrate into BC forming a multi-layer structure. This foam has a very well interconnected porous network structure. The X-ray diffraction patterns indicate that with the increase in chitosan content, the crystalline structure is not changed but the crystallinity index tends to decrease. The thermal degradation temperature increases from 263 to 366 °C with the chitosan content increasing from 12 to 45 per cent. The tensile test results show that the tensile strength and Young's modulus of BC–Chi composites tend to decrease with the increase in chitosan content but the value is much higher than that of pure chitosan. This improved elasticity of the BC–Chi composites is important for biomedical applications.

Keywords: composite materials, mechanical properties, bacterial cellulose, chitosan, crystallinity

1 INTRODUCTION

Bacterial cellulose (BC), which is synthesized by the *Acetobacter xylinum*, displays unique physical, chemical, and mechanical properties including a high crystallinity (70–90 per cent), a high water holding capacity (up to 200 times of its dry mass), and a well-developed surface area comprised of nanofibres, elasticity, mechanical strength, biodegradability, and biocompatibity. Being similar to human skin, BC can be applied as a skin substitute in treating extensive burns. Compared with other natural biodegradable polymers such as collagen, chitin, and gelatin, BC presents much higher mechanical properties. Several applications for BC in medical fields have already been reported, such as artificial skin for humans with extensive burns [**1**], artificial blood vessels for microsurgery [**2**], scaffolds for tissue engineering of cartilage [**3**], and wound dressing [**4**].

Chitosan, like BC, has been recognized for its applications in various fields including the biomedical area. It has been known for its absorption of exudes, antifungal, antimicrobial, antiviral, and wound-healing properties. Chitosan is useful as a wound management aid to reduce scar tissue. Chitosan has been also found to possess beneficial biological properties including haemostasis [**5**], antimicrobial activity stimulation of healing [**6**], tissue-engineering scaffolds [**7**], cell culture [**8**], and drug delivery [**9**]. However, the mechanical properties of chitosan are not enough to be used for biomedical applications. Thus, it is advantageous to make bacterial cellulose–chitosan composite (BC–Chi) materials for medical applications. Characterization of the structural parameters of BC–Chi composite materials with regard to their medical application has been studied [**10**]. BC has been modified in a form of hydrogel during microbial synthesis under static conditions with the use of the acetic bacterium *A. xylinum*. However, they have not investigated the chitosan content effect on

*Corresponding author: Center for EAPap Actuator, Department of Mechanical Engineering, Inha University, 1253 Yonghyun-Dong, Nam-ku, Incheon 402-751, Republic of Korea.
email: jaehwan@inha.ac.kr

the crystallinity, thermal stability, and mechanical properties of BC–Chi composite materials.

The aim of this study is to prepare a composite of BC and chitosan for potential biomedical application such as wound dressing or scaffold in tissue engineering by post-modification in an attempt to use the synergic beneficial aspects of both polymers. In the beginning, we study the effect of chitosan content on the morphology of scaffold, crystallinity, thermal stability, and mechanical properties of the composites. The antibacterial properties and biocompatibility test are ongoing.

2 EXPERIMENTS

Gluconacetobacter xylinum BRC-5 was obtained from Yonsei University and used to produce the BC pellicles. The bacterium was cultured on Hestrin and Schramm (HS) medium, which was composed of 2 per cent (w/v) glucose, 0.5 per cent (w/v) yeast extract, 0.5 per cent (w/v) bacto-peptone, 0.27 per cent (w/v) disodium phosphate, and 0.115 per cent (w/v) citric acid. All the cells precultured in a test tube containing a small cellulose pellicle on the surface of the medium were inoculated into a 500 mL Erlenmeyer flask containing 100 mL of the HS medium. The flasks were incubated statically at 30 °C for 14 days. The BC pellicles were dipped into 0.25 M NaOH for 48 h at room temperature in order to eliminate the cells and components of the culture liquid. The pH was then lowered to 7.0 by repeated washing with distilled water. The purified BC pellicles were stored in distilled water at 4 °C to prevent drying [**11**].

The wet BC pellicles were placed between two sheets of filter paper to soak free water. Then, two pellicles were immersed in the chitosan-dissolved acetic acid solution (concentration of 1 per cent) for 15 and 45 min, coded as BCC-1 and BCC-2; two pellicles were immersed in the chitosan-dissolved acetic acid solution (concentration of 1.5 per cent) for 30 and 60 min, coded as BCC-3 and BCC-4 in room temperature, followed by soaking the excess chitosan solution by using filter paper. Finally, it was dried by using a freeze-dryer (IP3 Jouan, France) at −40 °C for 3 days. The pure BC pellicles were used as control sample and coded as BC.

Scanning electron microscope (SEM) images of BC and BC–Chi composites were taken with a SEM equipment (Hitachi S-4200, Japan) to study the morphological changes. The surface and cross-section of the samples were sputtered with gold, and SEM images were taken.

Fourier transform infrared spectrometer (FT–IR) spectra were obtained by using a Perkin–Elmer System 2000 FT–IR spectrophotometer. The composites were cut into very small particles and characterized by an FT–IR for the evaluation of chemical structures using a KBr pellet. The obtained data were transferred to the PC for the line fitting.

The X-ray diffraction (XRD) patterns were recorded on an X-ray diffractometer (D/MAX-2500, Rigaku), by using Cu Kα radiation at 40 kV and 30 mA. The diffraction angle ranged from 5° to 40°.

Thermo-gravimetric analysis (TGA) was carried out with an NETZSCH STA 409 PC/PG system. All analyses were performed with a 10 mg sample in aluminium pans under a dynamic nitrogen atmosphere between 30 and 1000 °C. The experiments were run at a scanning rate of 20 K/min.

Tensile test specimens were prepared by cutting the BC–Chi composites to 10 mm wide and 65 mm long strips using a precise cutter. Young's modulus of samples were found from the tensile test results conducted according to ASTM D-882-97 as a standard test method for tensile elastic properties of thin plastic sheeting. The tensile test was performed on a universal testing machine. Extension speed of the instrument was 2 mm/min. The test was performed in ambient condition.

3 RESULTS AND DISCUSSION

In the present study, the soft gel obtained by *A. xylinum* is treated with chitosan acetic acid solution, instead of being dehydrated. We expect that, by immersing the BC gel in chitosan solution, the multiple water layers surrounding chains would be displaced, resulting in bond formation between BC and chitosan. By changing the chitosan concentration from 1 to 1.5 per cent and immersion time from 15 to 60 min, four kinds of BC–Chi composites with different weight ratios have been prepared. Table 1 shows the weight ratio of the BC and chitosan in the composite and corresponding experimental condition. The chitosan content ranged from 12 to 45 per cent. Pure BC is used as a comparison sample.

Figure 1 presents surface and cross-sectional SEM images of freeze-dried BC and BC–Chi composites. As seen from Fig. 1(a), pure BC nanofibrils can be observed on the surface. The mean diameter of these nanofibrils is about 40 nm. From the cross-sectional image (Fig. 1(a)), multiple layer structures with a high aspect ratio and a well-organized three-dimensional

Table 1 Bacterial cellulose and chitosan content in the composite and the corresponding experimental condition

Code	Chitosan concentration (%)	Immersion time (min)	Bacterial cellulose content (%)	Chitosan content (%)
BCC-1	1	15	88	12
BCC-2	1	45	75	25
BCC-3	1.5	30	66	34
BCC-4	1.5	60	55	45

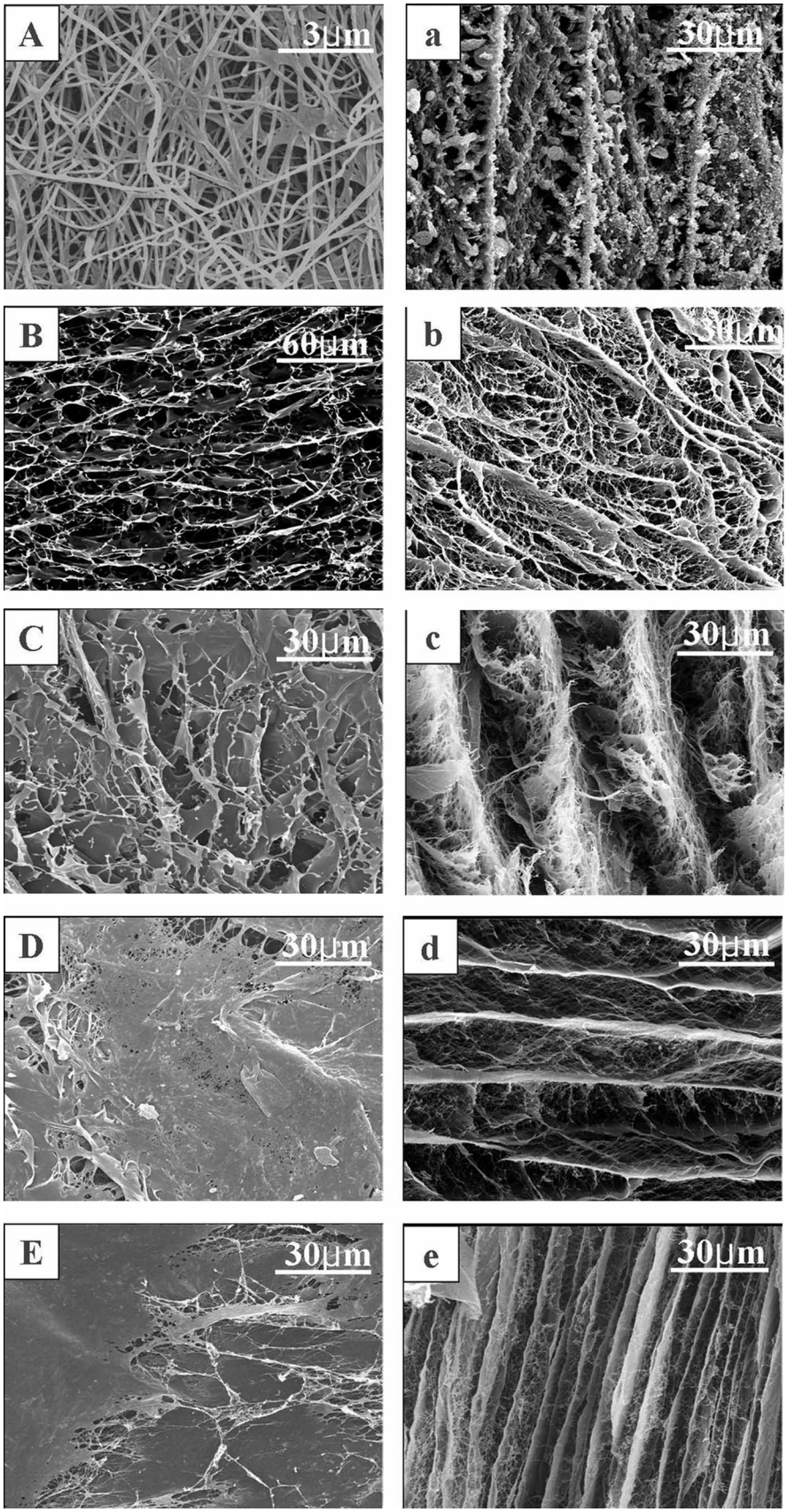

Fig. 1 SEM images of BC and BC–Chi composites (A, B, C, D, and E: surface images of BC, BCC-1, BCC-2, BCC-3, and BCC-4, respectively; a, b, c, d, and e: cross-sectional images of BC, BCC-1, BCC-2, BCC-3, and BCC-4, respectively)

(3D) network structure can be seen. The BC sample has porous morphology, which has been the subject of discussion in the last decade and already established. BC biosynthesis is characterized by unidirectional growth and crystallization, where glucose molecules are linear bonded by $\beta(1 \rightarrow 4)$-glycosidic bond. The union of glycosidic chains forms oriented microfibrils with intramolecular hydrogen bonds [**12**].

After treating with chitosan, some changes on BC–Chi composites happened both on the surface and cross-sectional morphology. A porous structure appeared on the surface of BC–Chi composites especially for low chitosan content. The reason for this is because chitosan remained on the surface after the treatment. This porous structure is a typical result for the freeze-drying method. When the chitosan content is as high as 45 per cent, the porous structure disappeared and a thick layer is formed due to the coverage of BC nanofibrils by chitosan (Fig. 1(e)). From the cross-sectional images, we can see that chitosan molecules can penetrate into BC and form a BC–Chi layer composite. For low chitosan content, such as 12 per cent, a porous structure still can be observed and the BC–Chi composite layer was very thin (Figs 1(c) and (d)). With the increase in chitosan content, the porous structure gradually disappeared due to the fact that chitosan filled the pores of BC composite and the distance between each layer also decreased. For all composites, BC nanofibrils can be observed between layers at which they are interconnected with each other. Note that the nanofibrous BC and BC–Chi composites have an interconnected porous network structure that has essentially large surface area and is useful for cellular attachment and vascularization. This BC–Chi composite can promote cellular ingrowth when it is used as tissue-engineering scaffolds.

Since the molecular structure of BC and chitosan is very similar, it is expected that these two polymers have good compatibility and miscibility. Figure 2 depicts the FT–IR spectra of BC and BC–Chi composite samples. In the case of pure BC, a broad band at 3450 cm^{-1} is attributed to O–H stretching vibration. Band at 2820 cm^{-1} represents the aliphatic C–H stretching vibration. A sharp and steep band observed at 1080 cm^{-1} is due to the presence of C–O–C stretching vibrations. In the case of BC–Chi composite, N–H stretching vibration band is located at 3420 cm^{-1}, which is combined with O–H stretching vibration band. Three new bands observed at 1647, 1575, and 1375 cm^{-1} are attributed to amide-I, amide-II, and amide-III, respectively, which exist in chitosan molecules.

Figure 3 shows the XRD pattern of the pure BC and BC–Chi composite samples. For pure BC, three main peaks located at 14.2, 16.6, and 22.4° can be identified in both spectra for (1 1 0), (1 1 0), and (2 0 0) reflexion planes of cellulose I [**13**]. For BC–Chi composites, peaks remained in the same location and only the peak

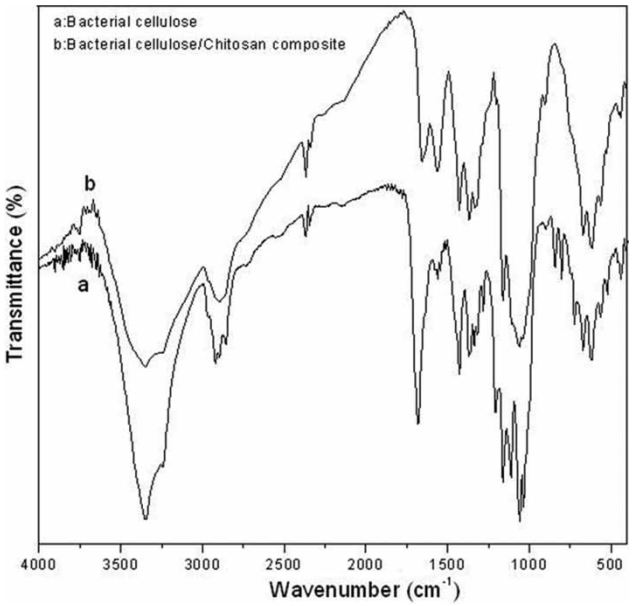

Fig. 2 FT–IR spectra of BC and BC–Chi composite (BCC-2)

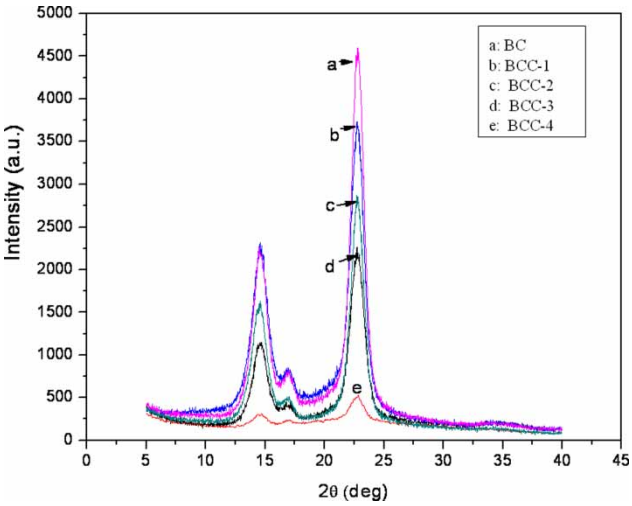

Fig. 3 The XRD patterns for BC and BC–Chi composites

intensities decrease sharply with the increase in chitosan content. This indicates that no changes on the crystalline structure occurred during the introduction of chitosan.

Crystallinity index can be calculated from XRD data according to the literature method [**14**]. This method is fast and easy. It uses the height of (2 0 0) peak and the minimum between (2 0 0) and (1 1 0) peaks, assuming that intensity of (2 0 0) represents both crystalline and amorphous parts, while the minimum intensity at the mentioned location is for amorphous part only

$$\mathrm{CrI} = \frac{(I_{(200)} - I_{(\mathrm{am})})}{I_{(200)}} \tag{1}$$

where CrI is the crystallinity, $I_{(200)}$ is the intensity at (2 0 0) peak ($2\theta = 22.3°$), and $I_{(\mathrm{am})}$ is the intensity at the minimum between (1 1 0) and (2 0 0) peaks.

The estimated crystallinity index with the variation of chitosan content is plotted in Fig. 4. For BC, the value is 87 per cent. For BC–Chi composites, it decreases from 83 to 61 per cent with the increase in chitosan content from 12 to 45 per cent. One reason may be due to a kind of intermolecular reaction between BC and chitosan, which makes BC molecular chains difficult to move. Another reason is that chitosan is an amorphous polymer. It may act as a diluent. Although it is an estimated crystallinity based on the XRD data, it is relevant to point out that the BC exhibited high crystallinity.

TGA is a continuous process, involving the measurement of sample weight in accordance with increasing temperature in the form of programmed heating. Since TGA provides better understanding of thermal decomposition behaviour, the thermal stability and thermal decomposition of BC and BC–Chi composite were investigated using TGA and are given in Fig. 5. The TGA curves obtained by plotting percentage weight loss against temperature indicate that BC is thermal stable up to a temperature of 220 °C.

Some important data such as the weight loss percentage at 250 °C and thermal degradation temperature at 50 per cent weight loss are plotted against chitosan content in the composite. The results are shown in Fig. 6. For pure BC, the weight loss at 250 °C is 24.2 per cent. For BBC-1 it decreases to 17.8 per cent. The weight loss at 250 °C decreases as the chitosan content increases, and becomes saturated after 25 per cent of chitosan content. In the case of thermal degradation temperature at 50 per cent weight loss, for pure BC it is noticed at 263 °C. However with the increase in chitosan content from 12 to 45 per cent, the value increases from 306 to 366 °C. All these results indicate that with the incorporation of chitosan, the thermal stability of the composite has been improved.

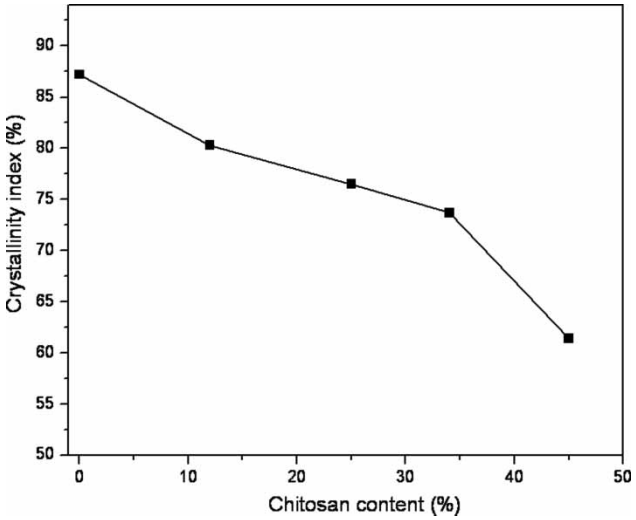

Fig. 4 The effect of chitosan content on the crystallinity index of BC–Chi composites

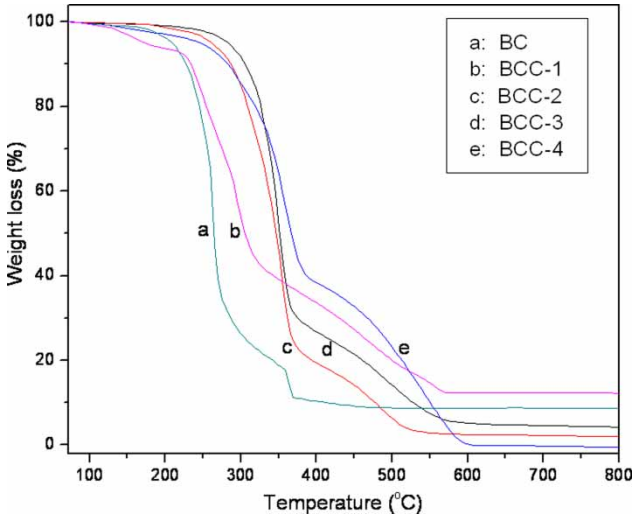

Fig. 5 TGA curves for BC and BC–Chi composites

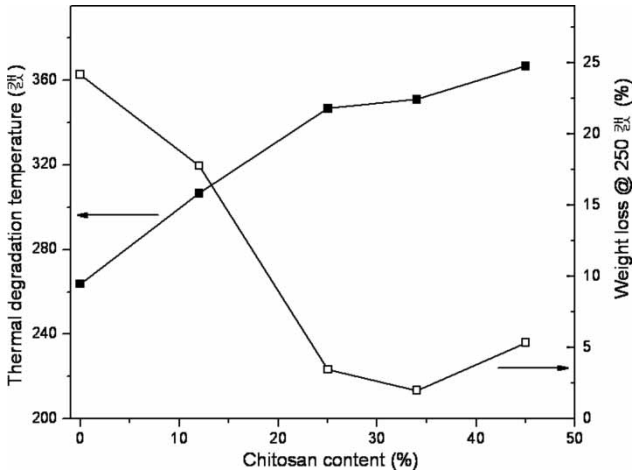

Fig. 6 The effect of chitosan content on the thermal degradation temperature and weight loss at 250 °C of BC–Chi composites

Thermal degradation temperature is affected by structural parameters such as molecular weight, crystallinity, and orientation. Note that the crystallinity of BC–Chi composite is lower than that of pure BC. The thermal degradation temperature of BC–Chi composite should be shifted to lower temperature. However the result is not consistent with the expectation. The reason for this might be because of the formation of some kind of intermolecular reaction between BC and chitosan, which can improve cohesive energy resulting in higher thermal stability.

Figure 7 shows the mechanical properties in terms of tensile strength, Young's modulus, and tensile strength calculated from stress–strain curves of the BC–Chi composites. All samples exhibit almost linear elastic behaviour from the beginning to the break point. No yielding point can be observed. For pure BC, the tensile strength and Young's modulus are 160 MPa and

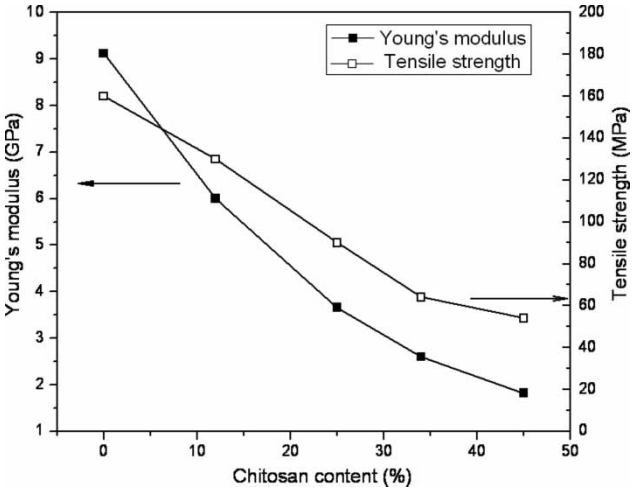

Fig. 7 Mechanical properties of BC–Chi composites

9.12 GPa, respectively. With the increase in chitosan content from 12 to 45 per cent, the tensile strength tends to decrease from 130 to 54 MPa and Young's modulus decreases from 6.0 to 1.8 GPa. These results indicate that the composites become resilient with the increase in chitosan content. This improved elasticity is important for biomedical application of BC because BC is too stiff to be applied for medical applications. Note that these mechanical properties, especially tensile strength and Young's modulus, are much higher than that of pure chitosan.

4 CONCLUSIONS

BC–Chi composites have been successfully prepared by immersing wet BC pellicle in chitosan acetic acid solution followed by freeze-drying. SEM images showed that these BC–Chi composites have a well-developed 3D porous network structure. Chitosan molecules can penetrate into BC forming a multi-layer network structure. With the introduction of chitosan in BC, the crystalline structure did not change but crystallinity greatly decreased with the increase in chitosan content. However thermal stability has been improved by the incorporation of chitosan. At the same time, tensile strength and the Young's modulus of BC–Chi composites decreased with the increase in chitosan content. But the value is much higher than that of pure chitosan. Since both BC and chitosan are biodegradable polymers, the BC–Chi composites might be useful for potential scaffold material in tissue engineering or other medical applications such as wound dressing, and so on.

ACKNOWLEDGEMENT

This work was supported by Creative Research Initiatives (EAPap Actuator) of KOSEF/MEST.

REFERENCES

1 **Fontana, J. D., de Sousa, A. M., Fontana, C. K., Torriani, I. L., Moreschi, J. C., Gallotti, B. J., de Sousa, S. J., Narcisco, G. P., Bichara, J. A.,** and **Farah, L. F.** Acetobacter cellulose pellicles as a temporary skin substitute. *Appl. Biochem. Biotechnol.*, 1990, **24/25**, 253–264.

2 **Klemm, D., Schumann, D., Udhardt, U.,** and **Marsch, S.** Bacterial synthesized cellulose-artificial blood vessels for microsurgery. *Prog. Polym. Sci.*, 2001, **26**, 1561–1603.

3 **Svensson, A., Nicklasson, E., Harrah, T., Panilaitis, B., Kaplan, D. L., Brittberg, M.,** and **Gatenholm, P.** Bacterial cellulose as a potential scaffold for tissue engineering of cartilage. *Biomaterials*, 2005, **26**, 419–431.

4 **Alvarez, O. M., Patel, M., Booker, J.,** and **Markowitz, L.** Effectiveness of biocellulose wound dressing for the treatment of chronic venous leg ulcers: results of a single center randomized study involving 24 patients. *Wounds*, 2004, **16**, 224–233.

5 **Pusateri, A. E., McCarthy, S. J., Gregory, K. W., Harris, R. A., Cardenas, L.,** and **McManus, A. T.** Effect of a chitosan-based hemostatic dressing on blood loss and survival in a mode of severe venous hemorrhage and hepatic injury in swine. *J. Trauma*, 2003, **54**, 177–184.

6 **Azas, A. K., Sermsintham, N., Chandrkrachang, S.,** and **Stevens, W. F.** Chitosan membrane as a wound-healing dressing: characterization and clinical application. *J. Biomed. Mater. Res. B, Appl. Biomater.*, 2004, **69**, 216–224.

7 **Di Martino, A., Sittinger, M.,** and **Risbud, M. W.** Chitosan: a versatile biopolymer for orthopedic tissue-engineering. *Biomaterials*, 2005, **26**, 5983–5989.

8 **Ayşe, G. K., Cristina, S., Menemşe, G.,** and **Giovanni, M.** Enhancement of fibroblastic proliferation on chitosan surface by immobilized epidermal growth factor. *Acta Biomater.*, 2008, **4**, 989–995.

9 **Aksungur, P., Sungur, A., Unal, S., Iskit, A. B., Squier, C. A.,** and **Senel, S.** Chitosan delivery system for treatment of oral mucositis: *in vitro* and *in vivo* studies. *J. Control Release*, 2004, **98**, 269–275.

10 **Ciechanska, D.** Multifunctional bacterial cellulose/chitosan composite materials for medical applications. *Fibres Text. East. Eur.*, 2004, **12**(4), 69–72.

11 **Seok, H. Y., Jin, H.-J., Kook, M.-C.,** and **Yu, R. P.** Electrically conductive bacterial cellulose by incorporation of carbon nanotubes. *Biomacromolecules*, 2006, **4**, 1280–1286.

12 **Saxena, I. M., Kudlicka, K., Okuda, K.,** and **Brown Jr, R. M.** Characterization of genes in the cellulose-synthesizing operon (acs operon) of *Acetobacter xylinum*: implications for cellulose crystallization. *J. Bacteriol.*, 1994, **176**, 5735–5741.

13 **Tokoh, C., Takabe, K., Fujita, M.,** and **Saiki, H.** Cellulose synthesized by *Acetobacter xylinum* in the presence of *Acetyl glucomannan*. *Cellulose*, 1998, **5**, 249–256.

14 **Segal, L., Creely, J. J., Martin, A. E.,** and **Conrad, C. M.** An empirical method for estimating the degree of crystallinity of native cellulose using the X-ray diffractometer. *Text. Res. J.*, 1959, **29**, 786–794.